Published in final edited form as:
Nano Lett. 2008 October ; 8(10): 3503–3509. doi:10.1021/nl080537r.

Encapsulation of Semiconducting Polymers in Vault Protein Cages

Benny C. Ng[1,4], **Marcella Yu**[2,4], **Ajaykumar Gopal**[1], **Leonard H. Rome**[3,4], **Harold G. Monbouquette**[2,4], and **Sarah H. Tolbert**[1,4,*]

[1]Department of Chemistry and Biochemistry, UCLA, Los Angeles, Los Angeles, CA 90095-1569, USA

[2]Chemical and Biomolecular Engineering Department, UCLA, Los Angeles, CA 90095-1592, USA

[3]Department of Biological Chemistry, David Geffen School of Medicine, UCLA, Los Angeles, CA 90095-1737, USA

[4]California NanoSystems Institute, UCLA, Los Angeles, CA 90095

Abstract

We demonstrate that a semiconducting polymer [poly(2-methoxy-5-propyloxy sulfonate phenylene vinylene), MPS-PPV] can be encapsulated inside recombinant, self-assembling protein nanocapsules called “vaults”. Polymer incorporation into these nano-sized protein cages, found naturally at ~10,000 copies per human cell, was confirmed by fluorescent spectroscopy and small-angle X-ray scattering (SAXS). Although vault cellular functions and gating mechanism remain unknown, their large internal volume and natural prevalence within the human body suggests they could be used as carriers for therapeutics and medical imaging reagents. This study provides the groundwork for the use of vaults in encapsulation and delivery applications.

Novel opportunities for nanomaterial assembly can be found by integrating biology, chemistry, and materials science. Biological templates such as DNA, protein fibers, protein cages or viral capsids can be used to form new composite materials with potential applications in drug delivery.[1-3] To produce a drug delivery system from these components, however, there must be a means to encapsulate desired cargo and then release it in response to biological stimuli. While viruses[4], synthetic biopolymers[5], and liposomes[6] have been the primary candidates for drug delivery systems[7], the naturally occurring bio-nanocapsule know as a “vault” is another attractive system for delivery. Vault particles are already present in human cells in high copy number[8], and their hollow barrel-like structure with a large internal volume seems well suited for encapsulation.

In this work, the ability of vaults to encapsulate fluorescent macromolecules as the first step toward delivery and bioimaging was investigated. The interior of the vault cage can be filled with an optically active polymer. Fluorescence spectroscopy and quenching measurements were utilized to explore changes in the polymer’s local environment and the nature of its association with vault particles. This was complemented by small angle X-ray scattering (SAXS), which was used to provide direct structural characterization of the vault/polymer composite in solution.

Vaults are abundant and conserved in most eukaryotes, including humans and rats, which reduce the probability of immunogenic effect.[9] In fact, they are the largest cytoplasmic

*Corresponding author. E-mail: tolbert@chem.ucla.edu.

ribonucleoproteins, forming massive complexes of molecular weight ~13 MDa.[10] Their cellular functions and gating mechanism are not yet understood.[10] Vaults have been implicated in nucleocytoplasmic transport because they localize to the nuclear pore complex and have been found associated with microtubules.[11-14] The above factors and their ability to remain intact after uptake into HeLa cells make them good candidates for delivery applications.[15]

Vaults are composed of four components. Vaults contain 96 copies of the 100-kDa major vault proteins (MVP), the 193-kDa vault poly(ADP ribose) polymerase (VPARP), the 290-kDa telomerase-associated protein 1 (TEP1), and untranslated vault RNA.[10] The 96 copies of MVP account for ~74% of the protein mass, and recombinantly synthesized MVP can self-assemble into a vault-like structure without the remaining components.16 This hollow cylindrical capped-barrel structure is measured to be 41 nm in diameter and 72.5 nm in length.16 Each vault contains two identical cup-like halves made of 48 copies of MVP.

When vaults are deposited onto a poly-L-lysine-coated mica surface, both open and closed conformations are observed using freeze-etch electron microscopy with platinum shadowing.[10] The closed structure represents the full vault while the open one occurs when vaults separate into their component halves, which in turn further open up into a flower-like structure composed of eight petals (6 MVPs per petal). The ease of transition to an open conformation indicates that vault complexes, while in solution, may have weakly bonded and potentially fluctuating quaternary structures. Consistent with this idea, they have been shown to dissociate into two halves in solution at pH < 4.[17] Furthermore, it is clear that moderate sized solute molecules can readily access the vault interior even at neutral pH. For example, thrombin, a 34-kDa protein, has been shown to access the interior of MVP-only recombinant vaults in the presence of a MVP interacting protein which contains a thrombin cleavage site.18

The present work uses two types of vaults: “regular” CP-MVP vaults (i.e., cystein-rich peptide-tagged MVP-only recombinant vaults) and “crosslinked” CP-MVP vaults, which have additional covalent tethers (EGS – ethylene glycol disuccinate di(N-succinimidyl) ester) between protein monomers to seal the vault cage.16,19,20 Both regular and crosslinked vaults are used to encapsulate the polyanionic semiconducting polymer poly(2-methoxy-5-propyloxy sulfonate phenylene vinylene) [MPS-PPV].

MPS-PPV is a π-conjugated polymer with alternating single and double bonds along the polymer backbone. Electrons in the π-orbitals delocalize over many monomers, forming a chromophore which strongly absorbs and fluoresces visible light. The photophysical properties of the polymer enable its use as electrochemical sensors, light-emitting diodes, and biological sensors.[21-24] While simple polymers like polystyrene sulfonate (PSS) have recently been encapsulated in viral protein shells,[25] the intrinsic fluorescence of MPS-PPV and its strong dependence on the local environment make it an excellent tool to study bio-composites.[26-28]

In solution, the fluorescent efficiency of MPS-PPV is linked to the physical conformation of its molecules, which in turn varies with solvent quality.[29] When the polymer is dissolved in a polar aprotic solvent such as DMSO (dimethyl sulfoxide, κ = 48 at 20 °C), the chains have open and extended structures. In contrast, the chains coil up in protic solvents such as water (κ = 80.1 at 20 °C). Compared to the coiled up structure, the extended structure has a red-shifted emission spectrum and enhanced fluorescence intensity. This is related to a longer conjugation length and reduced inter- and intra-chain energy transfer in DMSO solutions which in turn leads to reduced non-radiative relaxation. Moreover, like many polyelectrolytes, light scattering shows that chains further aggregate in water upon the

addition of salts.[30] The cations act as linkers and bring the polymer chains together, further reducing fluorescence intensity. MPS-PPV was thus chosen over other semiconducting polymers because it is water soluble, commercially available, and its photophysical properties are highly sensitive to the polymer environment.[28-30]

Polymer/vault complexes were produced simply by incubating the polymer with the vaults at room temperature in 20 mM 2-(N-morpholino)ethanesulfonic acid (MES) buffer at pH 6.5. The final polymer concentration was 10 μg/ml. Figure 1 compares emission spectra of MPS-PPV in three different buffers and as a mixture with CP-MVP vaults. The buffers vary in the ratio of DMSO to 20 mM MES. Steady-state fluorescence experiments were performed on a JY-Horiba Fluorolog-3. In the absence of vaults, the emission from MPS-PPV intensifies with increasing amount of the better solvent, DMSO, in the MES buffer. For the vault/MPS-PPV mixture in MES buffer, the emission red-shifts and intensifies, mimicking the effect of adding DMSO and leading to a near overlap of the spectrum with that for MPS-PPV in 20% DMSO. The addition of MPS-PPV does not alter the vault dimension or morphology as confirmed by the transmission electron microscope (TEM) images (JEM1200-EX, JEOL, Tokyo) in Figure 2a and 2b. To generate the images in Figure 2, a drop of the sample was placed on a carbon-coated copper grid and incubated for 5 minutes. The excess solution was then removed by lightly blotting the grid on a filter paper, following which the sample was negatively stained with 1% uranyl acetate and dried before imaging.

The intensity shifts presented in Figure 1 indicate that the environment of the polymer changes considerably with the addition of DMSO or vaults. When the fraction of organic solvent was increased, an expected increase in fluorescence intensity was seen accompanied by a red-shifted spectrum. Similarly, addition of vaults (instead of DMSO) to the polymer solution intensifies and red-shifts the polymer fluorescence. This suggests that when mixed with vaults, a detectable fraction of the polymer is in close association with a lower dielectric environment – the only possibility being association with the protein. Although the above trends suggest that the polymer has an affinity for the vaults, it does not reveal whether the affinities are similar for both the interior and exterior vault surfaces. The TEM images of the polymer/vault mixtures (Figure 2) suggest that no significant amount of polymer adsorbs on the vault exterior, but more proof is needed. If some fraction of the polymer is closely associated with the vault as suggested above, one would also expect a difference in its accessibility to solution based quenchers. Fluorescence quenching studies were thus conducted to further illustrate the interaction of the polymer with the vaults.

Conjugated polymers exhibit a superquenching effect, where because of rapid energy transfer, multiple chromophores along the backbone can be concurrently quenched by a single quencher molecule. Measuring changes in quenching efficiency therefore provides a very sensitive probe of conformation and therefore the dielectric environment seen by the polymer.[27-28,30] Polymer incorporation was examined using fluorescence quenching of MPS-PPV by the cationic quencher methyl-viologen (MV^{2+}) in the presence and absence of vaults. A Stern-Volmer relationship can be established to describe quenching efficiency using Equation 1 where K_{sv} is the Stern-Volmer constant, [Q] is the concentration of quencher, and Φ_o and Φ are quantum yields of the fluorophore with and without the quencher, respectively.[31] Quantum yields can be calculated using Equation 2 where I is the integrated fluorescence intensity, OD is the optical density, and n is the refractive index.[31] In this experiment, Rhodamine 6G in ethanol was used as a standard, and the fluorescence intensity was integrated from 470 to 800 nm.

$$\frac{\Phi_0}{\Phi} - 1 = K_{SV}[Q] \qquad \text{Equation 1}$$

$$\Phi_{sample} = \frac{OD_{std} \cdot I_{sample} \cdot \Phi_{std} \cdot n_{sample}^2}{OD_{sample} \cdot I_{std} \cdot n_{std}^2} \qquad \text{Equation 2}$$

A Stern-Volmer plot is shown in Figure 3. A steeper slope, K_{sv}, indicates better quenching efficiency. Methyl-viologen can easily bind to the polymer in buffer and quench its fluorescence in the absence of vaults (◆). In the presence of vaults (▲), a two-fold decrease in quenching efficiency was seen, indicating that at least some fraction of the polymer was associating with the vaults and thus some of the chromophors were not quenched. We hypothesize that the decrease in quenching efficiency is due to polymer adsorption to the vault complex and present evidence below that this occurs primarily at the inner vault surface.

When EGS crosslinked vaults are mixed with the polymers, the rigidified complex is expected to be less amenable to the entry of the polymer. If adsorption at the inner surface is prevented and that at the outer surface is minimal as proposed, no significant difference between the quenching in this system and that for free polymer in solution should be seen. Indeed the K_{sv} for a crosslinked vault/polymer mixture (■) is comparable to the K_{sv} for polymer without vaults (◆). This suggests little or no association of the polymer with crosslinked vaults. It follows that crosslinking, which involves multiple connections between protein monomers, must indeed exclude the polymer from the vault interior while maintaining low affinity to the outer surface. If, however, the polymer is allowed to associate with the vaults first and this is followed by chemical cross-linking, we expect that the polymer adsorbed inside the vault would be trapped in the associated configuration. In such a case, quenching levels similar to a vault/polymer mixture with no cross-lnikers would be expected. Surprisingly, the quenching constant for such a polymer encapsulated crosslinked vault/polymer mixture (●) drops even lower than for the regular vault/polymer mixture. This result suggests that crosslinking may also inhibit quencher access to the vault interior. Figure 2c shows that the morphology of vaults remains unaffected by this process. In summary, the quenching studies presented above confirm that MPS-PPV is predominantly associated with the vault interior and crosslinking is a good strategy to seal off the interior of the vault to trap the cargo and control the access of surrounding solutes.

To confirm the above scenario, direct structural information, in the form of radial electron density distributions, was obtained using small angle X-ray scattering (SAXS). For dilute solutions, SAXS profiles yield the form factor of the scattering object. In this case, the scattering pattern arises from coherent scattering from correlated electron density within the object. The scattering measurements were performed at the Stanford Synchrotron Radiation Laboratory (beamline 4-2). For the experiment, 25 μl of each sample was held at 25°C in a quartz capillary. Scattered X-rays were collected (λ = 1.38 Å, 20 scans of 30 s each) on a MarCCD detector as 512 × 512 pixel images with a sample-to-detector distance of 2.5 m. The images were radially averaged to obtain one dimensional scattering curves.

The form factor, I(q), was obtained by subtracting the buffer scattering from that of the sample. The observable q range was 0.006 to 0.25 $Å^{-1}$. The distance distribution function, P(r), was computed as the inverse Fourier transform of I(q) within the limits of r set by the q range. The P(r) curve represents the radially averaged distribution of electron density

correlations (i.e., scattering length density) at a separation of r within the object. The collected data were analyzed using the ATSAS package.32–34 Based on concentration series data, the vault concentration of 1.5 mg/ml was chosen for all SAXS measurements to eliminate inter-particle interference (i.e., structure factor effects).

P(r) data thus provides a direct measure of vault conformation and gives information about the location of guest species. The distance distributions of two different types of vaults are shown in Figure 4. The asymmetric shape of the CP-MVP P(r) curve (- - - line) corresponds to a hollow shell structure. In analogy with ellipsoidal shells, we expect the maximum at ~350 Å to represent the diameter of the short axis of the vault. Preliminary calculations of P(r) from cryo-EM electron density maps[35] confirm that the profile of the solid black curve is as expected for a vault-like ellipsoidal shell. An increase in probability at length scales smaller than 350 Å would then corresponds to inclusion of materials into the vault interior.

To verify the ability of SAXS measurements to detect the inclusion of material into the vault, an established protocol of inclusion of a 55-kDa protein was used as a control.15 The protein has a 254 amino acid sequence which is known to bind on the inner surface of the vault at a region called the “int” domain. Although the number of int-tagged proteins inside this vault sample is unknown, multiple copies of the proteins have been shown to bind to the vault interior using cryoTEM[17] and gas-phase electrophoretic molecular analysis (GEMMA) (Catherine Kaddis et. al., unpublished). The P(r) of the protein-conjugated mixture (Fig 4. — line) shows a clear increase in scattering length density between 200 Å and 350 Å. Beyond 400 Å, the two curves overlap, confirming the absence of protein-conjugation on the vault exterior and the viability of SAXS as a sensitive technique capable of detecting the inclusion of material into the vault cage.

As SAXS appears to be sensitive to molecular binding in the vault interior, we then moved on to the semi-conducting polymer system. Figure 5 compares P(r) of pure polymer, vault proteins, and the mixture of the two in the same stoichiometry as in the quenching studies. The pure polymer (… line) scatters weakly and exhibits a broad P(r). The vault curve (- - - line) shows the typical CP-MVP P(r) as seen in Figure 4. The mixture (— line) containing CP-MVP and MPS-PPV, however, shows a small but significant increase in P(r) between 150 Å and 350 Å. Beyond 400 Å, the curves for the vaults and the mixture are identical within experimental error. The above data suggests that, similar to the int-tagged protein, the majority of the mass of MPS-PPV associated with the vault cage is in its interior. In both cases, the probability increases only between 150 Å and 350 Å. This data supports the deduction from the quenching studies that MPS-PPV is primarily located in the vault interior.

Another parameter that is sensitive to whether the polymer is inside or outside the vault is the radius of gyration (R_g). The radius of gyration, more precisely $\langle R^2 \rangle^{1/2}$ for the ensemble of objects in the sample (Equation 3), is computed from the normalized second moment of the distance distribution with respect to the center of mass.[34]

$$R_g^2 = \langle R^2 \rangle = \frac{\int_0^{D_{\max}} P(r)\, r^2 dr}{2\int_0^{D_{\max}} P(r)\, dr} \qquad \text{Equation 3}$$

The R_g of a vault, a measure of its compactness, is expected to decrease with inclusion of polymer inside, and increase if the polymer is adsorbed on the outer surface of the vault. Figure 6 shows the radius of gyration of vault/polymer mixture as a function of polymer-to-vault ratio. The ratio used in Figure 5 was arbitrarily set to unity. Variations on this ratio and

the corresponding R_g's are shown in Figure 6. The vault concentration is kept the same across all samples; only the polymer concentration is changed. The R_g's of both CP-MVP and EGS crosslinked vaults without any polymer was ~ 228 Å. When a small amount of the polymer was added (polymer/vault = 0.5), the R_g of the CP-MVP sample decreased by ~ 7 Å. Further addition of the polymer led to a monotonic increase in R_g. In contrast, the initial decrease in R_g was not observed for the EGS crosslinked vaults. The above data suggests that at a low polymer/vault ratio, there is a preferential inclusion of the polymer into regular vaults and this is prevented by EGS crosslinking. The increase in R_g with increase in the polymer/vault ratio is attributed to non-specific adsorption of the polymer to the exterior as well as an increase in the background scattering from the free polymer (R_g ~ 260 Å).

Together, all of these results provide strong evidence that vaults can encapsulate semiconducting fluorescent polymers. A final question, however, is to what extent is this encapsulation driven simply by mass action, or is there a strong interaction between the anionic polymer and vault cage that facilitates encapsulation? To investigate this mechanistic aspect of incorporation, a centrifugation experiment was performed on the polymer/vault mixture. After the polymer/vault mixture (3 ml total volume) was incubated for 30 minutes, the fluorescence intensity of the mixture was measured. Then, the vault particles were pelleted at 100,000 g for 1 hour, leaving any unbound polymer in supernatant. The top 2.5 ml was labeled supernatant and the bottom 0.5 ml was used for resuspension. The resuspension was diluted back to 3 ml, and the fluorescence intensity of the supernatant and the resuspended vaults was measured. Because some free polymer was likely included with the pellet in the bottom 0.5 ml of solution, all luminescence data was corrected for this free polymer by assuming that the bottom 0.5 ml has the same free polymer concentration as the top 2.5 ml and subtracting this value from the measured luminescence of the resuspended pellet. The centrifugation process for the vaults pellet solution was repeated for two more cycles, and the fluorescence intensity for the supernatant and the resuspended pellet solution were measured at each point.

Figure 7 shows the integrated fluorescence intensity of the supernatant and the resuspended pellet as a function of centrifugation cycle. The integrated fluorescence intensity of the supernatant at the zero cycle is the fluorescence intensity of polymer in buffer without vault particles. Likewise, the integrated fluorescence intensity of the resuspension at the zero cycle is the fluorescence intensity of vaults in buffer without any polymer. While the integrated fluorescence intensity of the supernatant decreases by about 80 times after 3 cycles, the integrated fluorescence intensity of the resuspended pellet decreases by only a small amount (~2x) and this decrease is likely due in part to sample loss during the centrifugation and resuspension process.. These data thus make two facts about the vault/polymer system clear. First, not all of the polymer is strongly associated with the vault particles at the concentration ratio used in the experiments. Second and more importantly, the polymer that is bound is strongly bound and can not easily be removed from the vault. This result thus provides strong evidence that polymer encapsulation in vaults does not depend on mass action or polymer concentration gradients, but is instead due to specific binding between the charged polymer and the vault.

The exact equilibrium binding constant unfortunately cannot be determined because the molecular weight of the polymer is unknown and could not be determined using standard methods due to the high affinity of the polymer for many gel or column matrices. Nonetheless, based on the data in figure 7, the binding affinity between the polymer and vaults appears to be large. We also performed another experiment to support the idea that polymer binding to the vault is an equilibrium process. In this case the many solutions produced in the centrifugation experiment was generated in a different manner. Instead of diluting the polymer through centrifugation, the same amount of vaults was incubated with

various MPS-PPV concentration for 30 minutes. Afterward, the fluorescence intensity was measured for each polymer/vault ratio. The integrated fluorescence intensity from this experiment (data not shown) was comparable with the intensity from the centrifugation experiment, a result that suggests equilibrium binding for both experiments.

Finally, from the centrifugation experiment described above, we can also estimate the amount of polymer bound to each vault particle. To do this, we quantified the extent to which vault binding enhances the luminescence of the polymer. Vault samples were incubated with progressively larger quantities of polymer, followed by luminescence measurements. The slope of the linear, low concentration portion of a plot of polymer concentration versus luminescence intensity was used to generate the enhancement factor. This value was then used to convert the luminescence from the pelleted sample in figure 7 into a polymer mass. Using this method, we estimate that approximately 8 μg of polymer are captured by each 100 μg of vaults.

Although we do not know the exact molecular interaction of the polymer with the vault exterior, the studies presented in this paper clearly demonstrate that polymer can be reliably encapsulated at low polymer/vault ratios. Unlike the case with the int-tagged protein, which was targeted into the CPMVP interior, the encapsulation of MPS-PPV does not rely on any specific protein binding domains engineered into the molecules in order to mediate encapsulation.[15] These results confirm that vaults are dynamic structures that allow facile encapsulation of macromolecules from their environment in the time scale of seconds to minutes.

While the electrostatic environment inside a vault is not completely understood, the ease of inclusion of MPS-PPV (an anionic polyelectrolyte) suggests the presence of a significant number of positively charged amino acids at the inner surface of vaults in contrast to the exterior. This prediction is also consistent with the fact that vault interiors are naturally found to encapsulate multiple copies of vault RNAs, which are polyanionic molecules. We note that varying ionic strength would be an ideal way to test this hypothesis of electrostatic interactions. Unfortunately, however, as mentioned above, the fluorescent efficiency of MPS-PPV is highly dependant on salt concentration.[30] For example, it was reported that adding just 1 mM $CaCl_2$ decreased the fluorescent efficiency of MPS-PPV by nearly 50%.[30] Thus, the interpretation of polymer/vault association at different ionic strengths would not be straight forward.

The biocompatibility of vaults and the ability to encapsulate and protect fluorescent materials inside provides a wide range of possibilities for vaults as inert markers for biological imaging. Moreover, understanding how to encapsulate macromolecules inside vaults and developing strategies to seal them is an important first step toward the use of vault protein cages as vessels for drug delivery. In future studies, major vault proteins could be modified for target specificity. Finally, probing polymer encapsulation in the vault interior will help us understand, by analogy, how other molecules might be sequestered in the vault interior. For example, our results indicate that a polymeric polyanionic drug should also be encapsulated inside the vaults in a manner similar to that used for MPS-PPV. If this drug could then be depolymerized using a pH change or external irradiation, the drug could then be released from the vault. One could imagine similar applications for gene therapy where large DNAs or RNAs carrying genetic information would constitute the vault cargo. In conclusion, we have demonstrated that vault protein cages can function as biological nano-capsules and can be loaded with non-biological molecular cargo. The results open up a range of potential applications for these nano-sized protein cages.

Acknowledgments

This work was supported by the National Science Foundation through a Nano-Science Interdisciplinary Research Team (NIRT) Grant (LHR, HGM, and SHT, MCB-0210690), an NSF IGERT Grant (BCN, DGE-0114443), and an instrumentation grant DMR-0114002. Additional support was provided by an NIH Biotechnology Training Award (MY, T32 GM067555), and by the California NanoSystems Institute. We thank Hedi Roseboro for preparing recombinant vault samples, Dr. Phoebe Stweart of Vanderbilt University for the schematic vault model, and Marc Niebuhr for technical assistance with SAXS studies. Portions of this research were carried out at the Stanford Synchrotron Radiation Laboratory, a national user facility operated by Stanford University on behalf of the U.S. Department of Energy, Office of Basic Energy Sciences. The SSRL Structural Molecular Biology Program is supported by the Department of Energy, Office of Biological and Environmental Research, and by the National Institutes of Health, National Center for Research Resources, Biomedical Technology Program.

References

1. Kudo H, Fujihira M. IEEE Trans Nanotechnol 2006;5:90.
2. Scheibel T, Parthasarathy R, Sawicki G, Lin XM, Jaeger H, Lindquist SL. PNAS 2003;100:4527. [PubMed: 12672964]
3. Allen M, Bulte JWM, Liepold L, Basu G, Zywicke HA, Frank JA, Young M, Douglas T. Magn Reson Med 2005;54:807. [PubMed: 16155869]
4. Cattaneo R, Miest T, Shashkova EV, Barry MA. Nature Rev Microbio 2008;6:529.
5. Kuskov AN, Shtilman MI, Goryachaya AV, Tashmuhamedov RL, Yaroslavov AA, Torchilin VP, Tsatsakis AM, Rizos AK. J Non-Cryst Solids 2007;353:3969.
6. Di Paolo D, Pastorino F, Brignole C, Marimpietri D, Loi M, Ponzoni M, Pagnan G. Tumori 2008;94:246. [PubMed: 18564613]
7. Torchilin VP. Annu Rev Biomed Eng 2006;8:343. [PubMed: 16834560]
8. Kickhoefer VA, Rajavel KS, Scheffer GL, Dalton WS, Scheper RJ, Rome LH. J Biol Chem 1998;273:8971. [PubMed: 9535882]
9. Kedersha NL, Miquel MC, Bittner D, Rome LH. J Cell Biol 1990;110:895. [PubMed: 1691193]
10. Kedersha NL, Heuser JE, Chugani DC, Rome LH. J Cell Biol 1991;112:225. [PubMed: 1988458]
11. Mikyas Y, Makabi M, Raval-Fernandes S, Harrington L, Kickhoefer VA, Rome LH, Stewart PL. J Mol Biol 2004;344:91. [PubMed: 15504404]
12. Goldsmith L, Yu M, Rome LH, Monbouquette HG. Biochemistry 2007;46:2865. [PubMed: 17302392]
13. Hamill DR, Suprenant KA. Dev Biol 1997;190:117. [PubMed: 9331335]
14. Chugani DC, Rome LH, Kedersha NL. J Cell Sci 1993;106:23. [PubMed: 8270627]
15. Eichenmuller B, Kedersha N, Solovyeva E, Everley P, Lang J, Himes RH, Suprenant KA. Cell Motility and the Cytoskeleton 2003;56:225. [PubMed: 14584025]
16. Slesina M, Inman EM, Moore AE, Goldhaber JI, Rome LH, Volknandt W. Cell Tissue Res 2006;324:403. [PubMed: 16505994]
17. Kickhoefer VA, Garcia Y, Mikyas Y, Johansson E, Zhou JC, Raval-Fernandes S, Minoofar P, Zink JI, Dunn B, Stewart PL, Rome LH. PNAS 2005;102:4348. [PubMed: 15753293]
18. Poderycki MJ, Kickhoefer VA, Kaddis CS, Ravel-Fernandes S, Johansson E, Zink JI, Loo JA, Rome LH. Biochem 2006;45:12184. [PubMed: 17002318]
19. Stephen AG, Raval-Fernandes S, Huynh T, Torres M, Kickhoefer VA, Rome LH. J Biol Chem 2001;276:23217. [PubMed: 11349122]
20. Yu M, Ng BC, Tolbert SH, Rome LH, Monbouquette HG. Nano Lett. co-submitted.
21. Ramanavicius A, Ramanaviciene A, Malinauskas A. Electrochimica Acta 2006;51:6025.
22. Gunes S, Neugebauer H, Sariciftci NS. Chem Reviews 2007;107:1324.
23. Rininsland F, Xia WS, Wittenburg S, Shi XB, Stankewicz C, Achyuthan K, McBranch D, Whitten D. PNAS 2004;101:15295. [PubMed: 15494445]
24. Kushon SA, Bradford K, Marin V, Suhrada C, Armitage BA, McBranch D, Whitten D. Langmuir 2003;19:6456.

25. Hu Y, Zandi R, Anavitarte A, Knobler CM, Gelbart WM. Biophys J 2008;94:1428. [PubMed: 17981893]
26. Douglas T, Young M. Nature 1998;393:152.
27. Achyuthan KE, Bergstedt TS, Chen L, Jones RM, Kumaraswamy S, Kushon SA, Ley KD, Lu L, McBranch D, Mukundan H, Rininsland F, Shi X, Xia W, Whitten DG. J Mater Chem 2005;15:2648.
28. Chen LH, McBranch DW, Wang HL, Helgeson R, Wudl F, Whitten DG. PNAS 1999;96:12287. [PubMed: 10535914]
29. Nguyen T-Q, Doan V, Schwartz BJ. J Chem Phys 1999;110:4068.
30. Smith AD, Shen CKF, Roberts ST, Helgeson R, Schwartz BJ. Res Chem Intermed 2007;33:125.
31. Lakowicz, JR. Principles of Fluorescence Spectroscopy. 2. Kluwer Academic/Plenum Pub.; New York, NY: 1999.
32. Konarev PV, Volkov VV, Sokolova AV, Koch MHJ, Svergun DI. J Appl Cryst 2003;36:1277.
33. Svergun DI. J Appl Cryst 1992;25:495.
34. Glatter, O.; Kratky, O. Small Angle X-ray Scattering. Academic Press Inc.; London: 1982.
35. Anderson DH, Kickhoefer VA, Sievers SA, Rome LH, Eisenberg D. PLoS Biology 5(11):e318.10.1371/journal.pbio.0050318 [PubMed: 18044992]

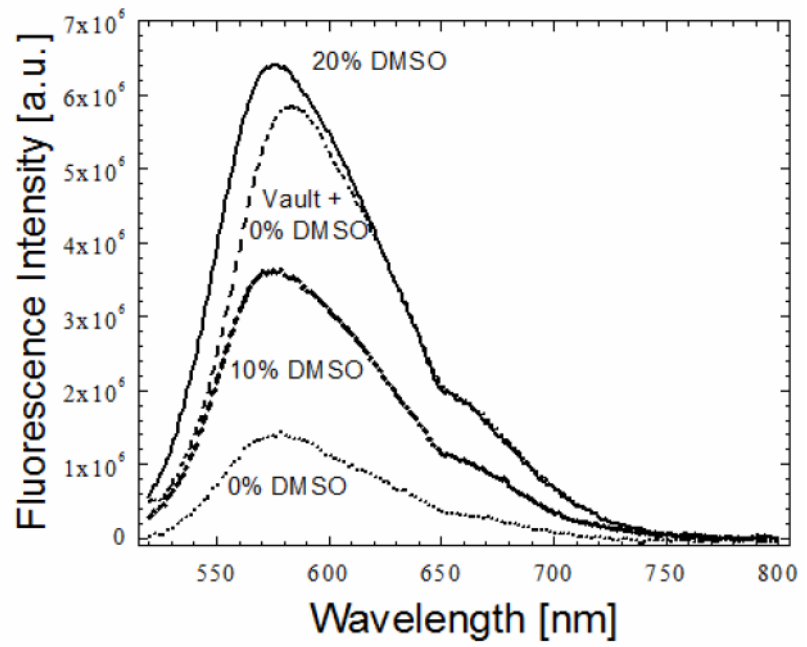

Figure 1.

Fluorescent spectra of MPS-PPV and vault/MPS-PPV mixture in different buffer conditions: (——— line) MPS-PPV in MES with 20% DMSO; (- - - - line) MPS-PPV in MES with 10% DMSO; (····· line) MPS-PPV in MES; (– – – – line) Vault/MPS in MES. The polymer concentration is 10 μg/ml in all the samples. The presence of the vault cage appears to produce an environment similar to 20% DMSO.

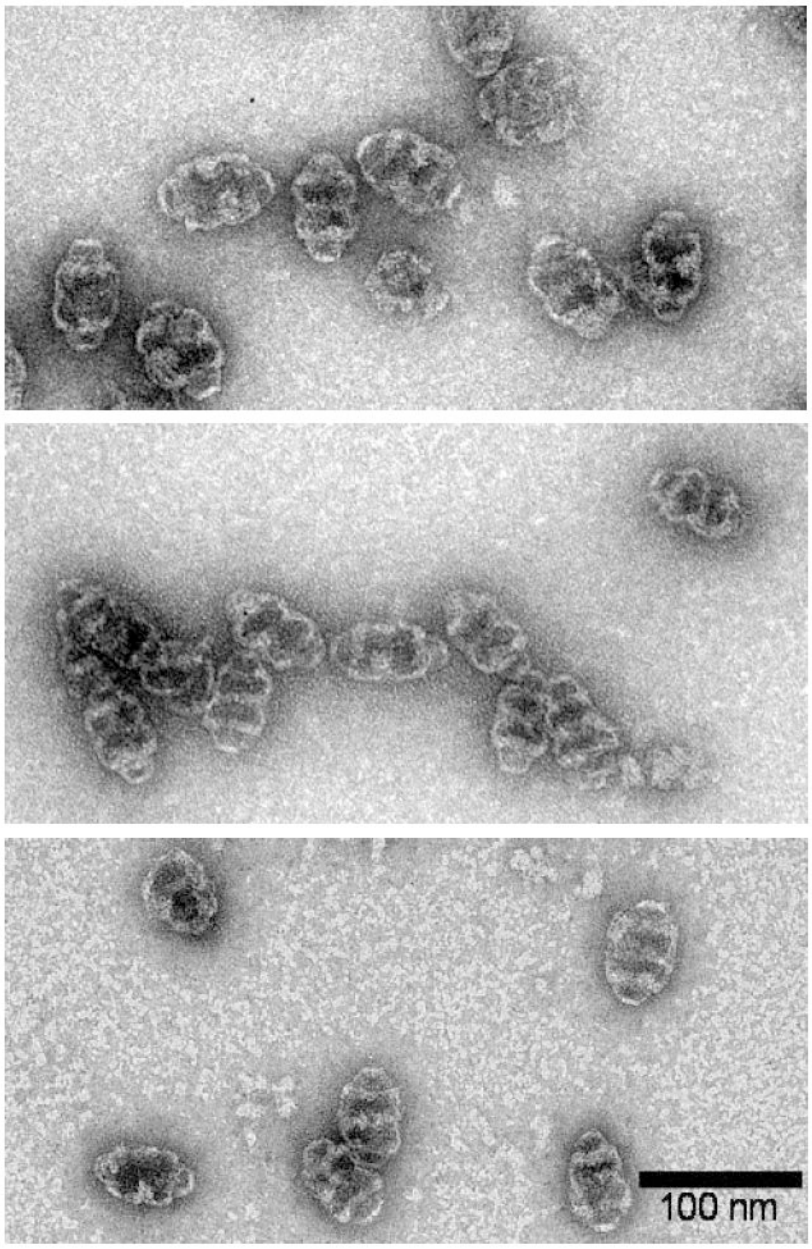

Figure 2.
Transmission electron microscope images of a) CP-MVP vaults, b) a CP-MVP vault/MPS-PPV mixture, and c) MPS-PPV inside EGS crosslinked vaults. In all cases, the standard vault structure is observed. Scale bar: 100 nm.

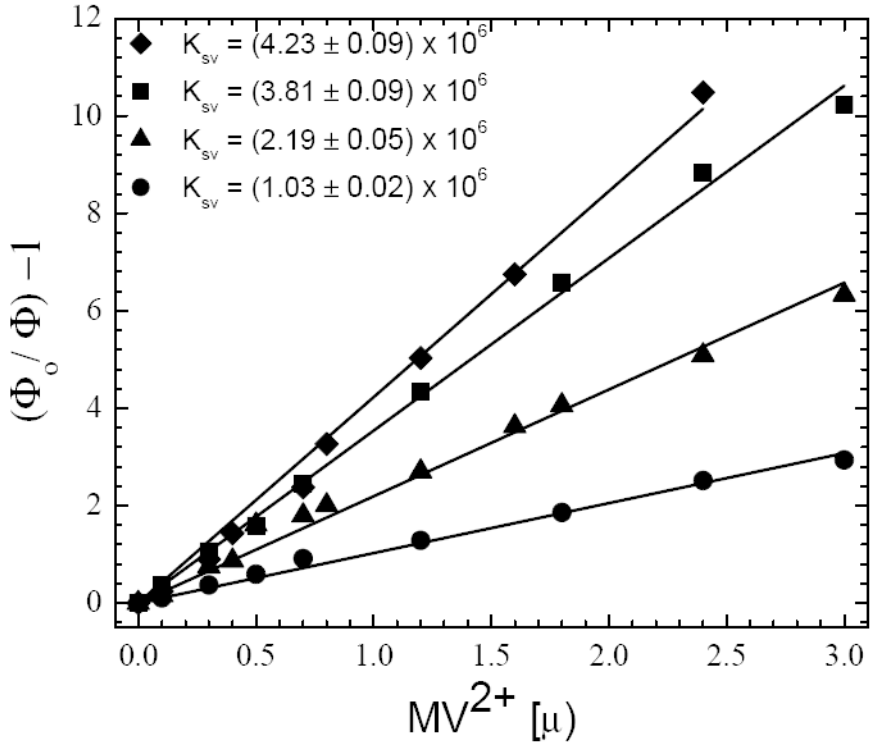

Figure 3.

Fluorescence quenching of MPS-PPV as a function of quencher (methyl viologen) concentration: ◆—MPS-PPV polymer only; ▲—vaults combined with MPS-PPV; ■—crosslinked vaults combined with MPS-PPV; ●—vaults combined with MPS-PPV and then subsequently crosslinked. Steeper slopes in the above Stern-Volmer plot indicate more effective quenching. The vault/polymer concentration ratio was constant for all the mixture.

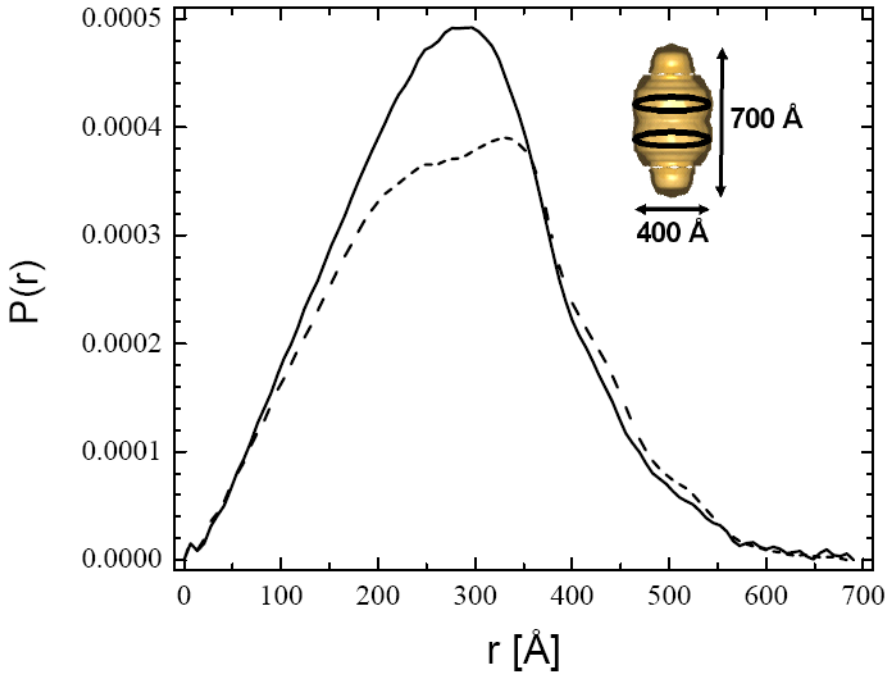

Figure 4.
The distance distribution, P(r), for CP-MVP (- - - line) and int-tagged CPMVP (— line) in 20 mM MES at pH 6.5. The protein concentration in both samples is identical. The two black circles in the vault schematic (inset) correspond to the expected binding site for the "int" protein.

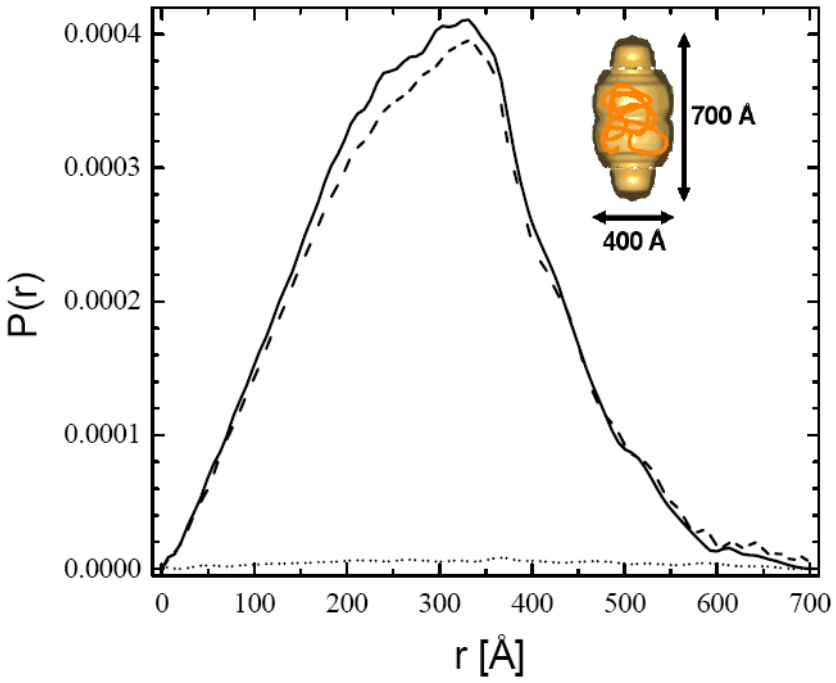

Figure 5.
Distance distribution, P(r), of vaults (— line), vault/MPS-PPV mixture (- - - - line), and MPS-PPV only (····· line). The protein and polymer concentration among samples are identical. All three samples were in 20 mM MES at pH 6.5.

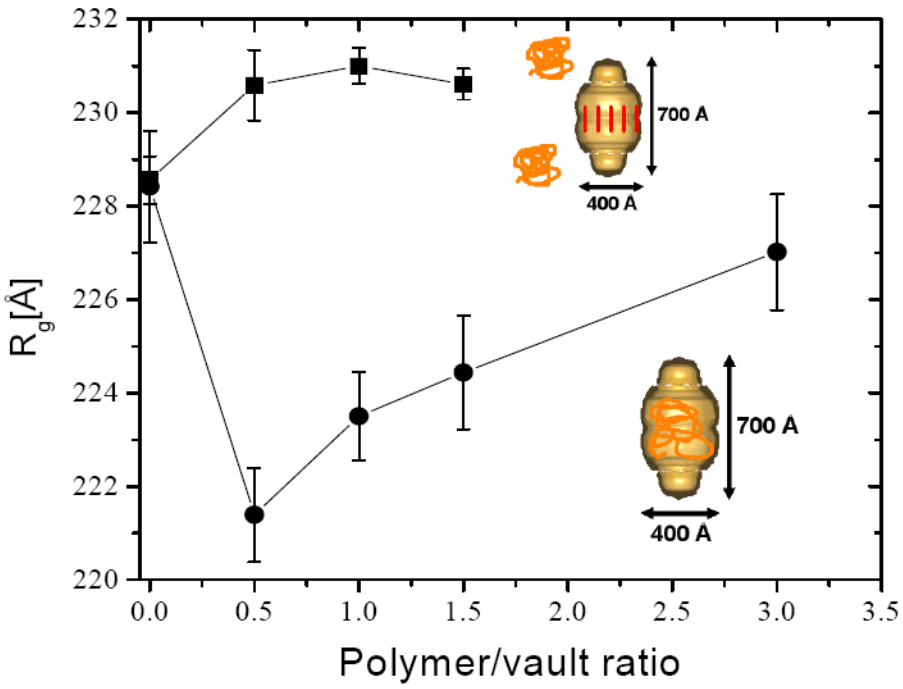

Figure 6.

Radius of gyration for vault/polymer mixture with different polymer:vault ratios: CP-MVP vaults (●), Crosslinked EGS vaults (■). The ratio of unity is arbitrarily set to the value used in figure 5 and represents a mixture with 7.5 μg polymer and 72.9 μg vault. The decrease in R_g at low ratios for uncrosslinked vaults is indicative of increased compactness in the polymer vault complex and is thus implies that the polymer is located in the vault interior.

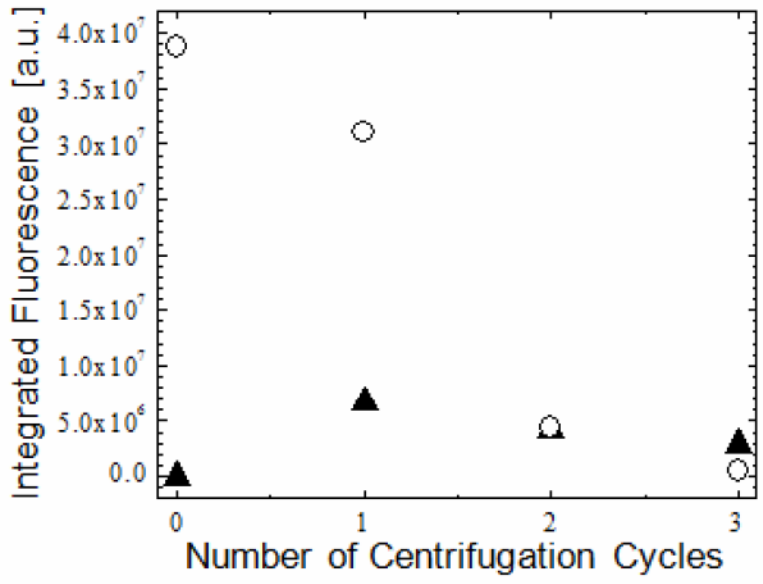

Figure 7.

Integrated fluorescence intensity as a function of centrifugation cycles: Supernatant (○), Resuspension (▲). The fluorescence intensity of the supernatant decreases by a factor of 80, while the fluorescence intensity of the resuspension decreases by only a factor of 2. The small decrease in luminescence intensity for the resuspended samples indicates that polymer encapsulation is not simply driven by polymer concentration gradient. Instead there appears to significant binding affinity between the polymer and the vault.